ACS Photonics

Article

pubs.acs.org/journal/apchd5

Strong Modification of Magnetic Dipole Emission through Diabolo Nanoantennas

Mathieu Mivelle,*[,†,#] Thierry Grosjean,[‡] Geoffrey W. Burr,[§] Ulrich C. Fischer,[⊥] and Maria F. Garcia-Parajo[†,∥]

[†]ICFO-Institut de Ciencies Fotoniques, Mediterranean Technology Park, 08860 Castelldefels, Barcelona, Spain

[‡]Department of Optics, FEMTO-ST Institute, UMR CNRS 6174, University of Franche-Comté, 25000 Besançon, France

[§]IBM Almaden Research Center, San Jose, California 95120, United States

[⊥]Interface Physics Group, Physics Institute, University of Münster, 48149 Münster, Germany

[∥]ICREA-Institució Catalana de Recerca i Estudis Avançats, 08010 Barcelona, Spain

ABSTRACT: Magnetic dipole transitions in matter are known to be orders of magnitude weaker than their electric dipole counterparts. Nanophotonic and plasmonic structures have the potential of strongly enhancing the optical magnetic fields in the near field, making these nanostructures ideal candidates to control and enhance the emission of magnetic dipole transitions. Here we theoretically investigate the potential of resonant optical nanoantennas based on diabolo and on metal−insulator−metal diabolo configurations to strongly modify the magnetic dipole of emitters. We find that both configurations provide unprecedented 10^2- to 10^3-fold enhancement of the total and the radiative decay rates of a magnetic dipole moment. We show that these two nanoantennas have opposed effects on the quantum yield of the magnetic dipole, translating into different antenna efficiencies. Furthermore, by using a magnetic dipole moment as a theoretical optical nanosensor, we numerically mapped the behavior of the magnetic local density of states (MLDOS) in the entire plane close to the diabolo nanoantenna. We demonstrate the strong confinement and local enhancement of the MLDOS by the nanoantenna. As such, these results underscore the unique ability of optical nanoantennas to control light emission from magnetic dipoles, opening new technological avenues in the magneto-optical domain.

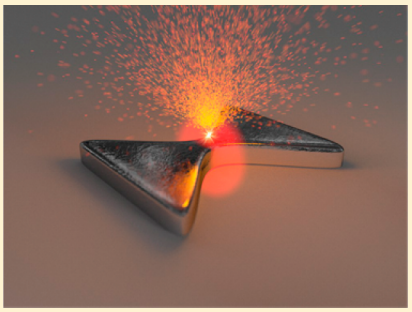

KEYWORDS: *nanophotonics, magnetic dipole transitions, diabolo optical antennas, magnetic local density of states*

The interaction between light and matter is widely considered being solely mediated by the electric field. This assertion also applies in the Bohr model, which holds that magnetic dipole transitions are about 10^5 times weaker than electric dipole transitions[1] and are therefore considered marginal. In this context, many researchers have aimed to control the spontaneous emission of electric dipole transitions through devices such as microcavities,[2] photonic crystals,[3] or optical antennas.[4,5] All of these approaches rely on the modification of the electric local density of states (ELDOS) in the vicinity of the considered electric dipole, characterized through the Purcell effect. Nowadays, this effect is commonly used to quantify the total decay rate enhancement of such electric dipole transitions, but it was originally employed to describe nuclear magnetic resonance decays.[6]

In parallel, it is also known that complex molecules have magnetic dipole moments in the optical domain. However, these optical transitions are extremely weak compared to their electric dipole transitions (about 10^2 to 10^5 times weaker[1,7]). In order to amplify the absorption and/or emission of these transitions, it is thus interesting to enhance the optical magnetic field together with the magnetic local density of states (MLDOS) around the molecules.

Recently, researchers have demonstrated that magnetic dipole transitions could also be studied in materials such as lanthanide[8,9] and metallic[10] ions. In these studies, it was shown that the MLDOS could be engineered in the same way as its electric counterpart.[11,12] In particular, the oscillating behavior of the MLDOS in space could be recorded in close proximity to metallic surfaces,[13] in good agreement with theoretical predictions. Nevertheless, only nonresonant structures have been experimentally used so far to study the MLDOS around such magnetic transitions. Resonant nanophotonic and plasmonic structures are known to strongly modify the behavior of electric[14−16] and magnetic[17−21] fields in the near field, making these nanostructures ideal candidates to strongly enhance the magnetic field of light.[22] These nanostructures could then actively control magnetic dipole transitions in matter. Indeed, it has been recently demonstrated theoretically that nanostructured dielectric[23] and metallic[24] materials could be used to modify locally the MLDOS. We therefore expect that tailored resonant plasmonic nanoantennas could be applied to significantly change the MLDOS near magnetic dipole

Received: March 16, 2015
Published: July 10, 2015

DOI: 10.1021/acsphotonics.5b00128
ACS Photonics 2015, 2, 1071−1076

transitions, leading to an increase of the magnetic fluorescence of the material carrying these transitions.

In this paper, we theoretically describe how to achieve unprecedented enhancement of both the total and radiative decay rates of a magnetic dipole moment by using resonant nanoantennas designed to strongly enhance the optical magnetic field of light in the near field at the telecom wavelength (λ = 1550 nm). We also show that these strong enhancements are magnetic dipole specific and are not related to an increase, in the same proportion, of the total and radiative decay rate of an electric dipole moment. Furthermore, we compare the effect on the quantum yield of the magnetic dipole moment of an optical nanoantenna alone as opposed to the so-called "sandwich" optical nanoantenna configuration, also known as the metal−insulator−metal (MIM) nanoantenna configuration.[25] Finally, we theoretically describe and quantify the modification of the MLDOS in the near field of a resonant optical nanoantenna by mapping the total decay rate in a plane situated in close proximity to the nanoantenna. Importantly, we demonstrate that resonant plasmonic nanoantennas are unique to strongly modify the emission of a magnetic nanosource at the nanometer scale, opening up new exciting possibilities in magneto-optics.

METHODS

We used finite difference time domain (FDTD) simulations to calculate the optical magnetic response of two different optical nanoantennas, a diabolo nanoantenna[22] (two metallic triangles connected by a metallic junction) and a sandwich diabolo nanoantenna (two diabolo nanoantennas superposed and separated by an insulator). The simulations consider a volume spanning ±2 μm in x, y, and z around the nanostructures. The optical nanoantennas are chosen to be in aluminum with a dielectric constant given by a Drude model at λ = 1550 nm. The antennas are located at $x = y = z = 0$ and are surrounded by air (optical index of 1). All six boundaries of the computational volume are terminated with convolutional-periodic matching layers[26] to avoid parasitic unphysical reflections around the nanostrcutures. The nonuniform grid resolution varies from 25 nm for areas at the periphery of the simulations to 5 nm for the region in the immediate vicinity of the antennas (±300 nm in x and y and ±150 nm in z). The excitation of the antennas is made by two different sources, depending of the type of studies: a plane wave or a magnetic dipole moment, as described later in this paper.

The total (Γ_{tot}) and radiative (Γ_{rad}) decay rate enhancements of the magnetic emitters placed in the vicinity of the optical nanoantennas are calculated and described by the equations

$$\Gamma_{tot} = \frac{P_{tot}}{P_0} \tag{1}$$

and

$$\Gamma_{rad} = \frac{P_{rad}}{P_0} \tag{2}$$

where P_{tot} and P_0 are the total powers emitted by the magnetic dipole with and without the optical nanostructures, respectively. P_{rad} is the power radiated in far-field in the presence of the optical antennas. These values are calculated at each position of the dipole with respect to the nanoantennas. For all the calculations, we consider that the magnetic dipoles have an intrinsic quantum yield of 1.

The quantum yield (η) of the magnetic nanosource is then obtained through the equation

$$\eta = \frac{\Gamma_{rad}}{\Gamma_{tot}} \tag{3}$$

RESULTS AND DISCUSSION

Our study is based on a diabolo optical nanoantenna, described previously by Grosjean et al.[22] and detailed in Figure 1. We explore two different nanoantenna configurations: (1) a single diabolo nanoantenna (Figure 1a), consisting of two metallic triangles separated by a metallic junction, and (2) the sandwich diabolo (S-diabolo) nanoantenna, made of two identical diabolos separated by an air gap of nanometric size (Figure 1b). The dimensions of these two configurations have been chosen such that the nanostructures generate a single magnetic hot spot at the metallic junction and at the telecom wavelength (λ = 1550 nm). The excitation is made with a plane wave launched 1 μm below the nanostructures, linearly polarized along the y-axis and propagating along the z-axis, as shown in Figure 1a and b. Figure 1c and d show the spectral responses of the diabolo and S-diabolo, respectively, calculated at a point centered on their metallic junction, 10 nm away from the metal. In this plane and at this position, the magnetic field is the strongest due to an intense electrical current flowing through the metallic junction under certain excitation conditions.[22] As clearly seen, both configurations enhance the magnetic field by more than 2 orders of magnitude (Figure 1c,d). Furthermore, the spectral response is broader for the diabolo antenna (Figure 1c) compared to the S-diabolo (Figure 1d), with quality factors of 4.18 and 7.28, respectively, at their resonances. These results indicate that the energy is stored more efficiently in the case of the MIM configuration and dissipated faster, mainly through radiative channels, in the case of the diabolo.

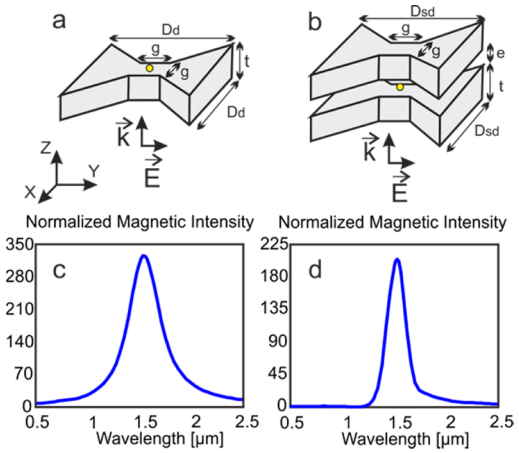

Figure 1. Antenna spectral responses. (a, b) 3D schematics of the diabolo (a) and S-diabolo (b) antennas, with t = 55 nm, g = 50 nm, e = 15 nm, D_d = 335 nm, and D_{sd} = 240 nm. The yellow point corresponds to the position where the spectra are calculated, 10 nm away from the antennas and centered on the metallic junctions. (c, d) Spectral magnetic intensity responses of the diabolo (c) and the S-diabolo (d). The vectors **k** and **E** represent the direction of propagation and the polarization of the electric field, respectively.

In order to compare the two configurations in terms of field enhancement and confinement, we calculated the normalized magnetic and electric field intensity distributions (H_{tot}^2/H_0^2

DOI: 10.1021/acsphotonics.5b00128
ACS Photonics 2015, 2, 1071−1076

and E_{tot}^2/E_0^2, respectively) in the *xy*-transversal and *xz*-longitudinal planes for each antenna under similar excitation conditions to those used for Figure 1a,b. H_{tot}^2, E_{tot}^2 and H_0^2, E_0^2 represent the magnetic and electric field intensity with and without the antenna, respectively. In agreement with previous reports,[22] we find that the magnetic field in the case of the diabolo antenna is localized around the metallic junction between the two metallic triangles (Figures 2a,e), whereas for

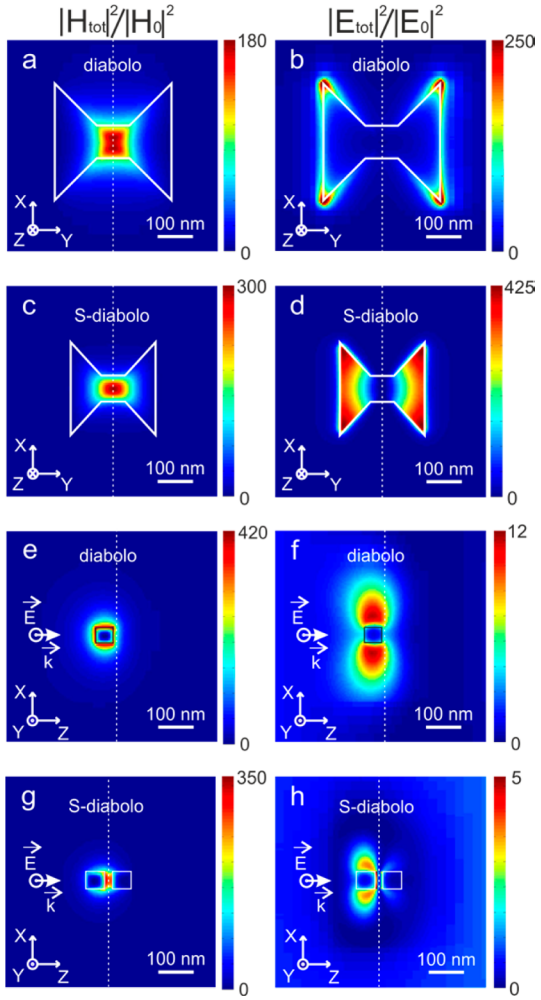

Figure 2. Normalized (a, c, e, g) magnetic and (b, d, f, h) electric intensity distributions in the case of (a, b, e, f) the diabolo and (c, d, g, h) the S-diabolo nanoantennas. The distributions are plotted in an *xy*-transversal plane, 10 nm away from the antennas (a–d), and in an *xz*-longitudinal plane (e–h), through the center of the metallic junction. The dashed lines in (a)–(d) represent the transversal planes shown in (e)–(h) and vice versa. The vectors **k** and **E** represent respectively the direction of propagation and the polarization of the electric field launched in the simulation. The solid lines surrounding the antennas are guides to the eyes.

the S-diabolo, the field is confined between the two metallic junctions of the two diabolos (Figure 2c,g). On the other hand, the electric field distribution for both structures is strongly delocalized toward the extreme parts of the antennas (Figure 2b,f for the diabolo and 2d,h for the S-diabolo) and do not overlap with the magnetic field distribution. Furthermore, the electric intensity is not confined into a small area, as its magnetic counterpart, although it still shows a certain degree of enhancement particularly in the *xy*-plane (Figure 2b), directly related to the magnetic field enhancement, as previously reported.[22] In the *xz*-plane, both the diabolo and S-diabolo configurations provide between 1 to 2 orders of magnitude higher enhancement of the magnetic field (Figure 2e,g) compared to the electric field (Figure 2f,h), underscoring the potential of these nanostructures to selectively magnify and confine magnetic fields.

Interestingly, the magnetic field intensity in the *xy*-transversal plane is higher and more confined in the case of the S-diabolo than in the diabolo (Figure 2a,c). Moreover, in the *xz*-longitudinal plane, the maximum of magnetic field intensity for the diabolo is slightly higher than for the S-diabolo (Figure 2e,g). This behavior is in apparent contradiction with studies reporting that sandwich structures are better suited for enhancing magnetic fields.[27,28] This effect can be understood by the fact that the diabolo is already a very efficient system to enhance the magnetic field and that coupling two diabolo antennas in air lowers the enhancement due to a screening effect of one of the diabolos with respect to the other. Notably, the magnetic field for the S-diabolo is significantly more confined than for the diabolo, with a mode volume of the electromagnetic energy density of about $(\lambda/16)^3$ nm^3 in the case of the diabolo and $(\lambda/30)^3$ nm^3 in the case of the S-diabolo. This higher degree of confinement is a direct effect of the coupling between the two diabolo nanoantennas.

Given the large enhancement of the magnetic field and its spatial delocalization with respect to the electric field, these plasmonic nanostructures should be well suited to locally control magnetic transitions in matter. To assess this possibility, we studied the effect of these two different nanostructures on the decay rates of point-like optical emitters described by a magnetic and an electric dipole moment. We performed a series of simulations by placing the dipole in the maximum of the magnetic field of each structure (i.e., near their metallic junctions) and then scanned the dipole along the antennas, as schematically shown in Figure 3a and b. Here, we assume that the dipole point source is a good approximation for a magnetic or electric dipole transition, as previously reported in the case of electric dipole transitions[29−31] described by electric dipole sources. The simulations consist of scanning the dipole along the three spatial dimensions in the case of the diabolo and in the transversal plane in the case of the S-diabolo (Figure 3a and b). For each position of the dipole with respect to the antennas, Γ_{tot} and Γ_{rad} are then calculated using eqs 1 and 2 and following the approach of Kaminski et al.[32] In this work the authors describe a method to theoretically calculate these values from an electric dipole. Γ_{rad} is measured by normalizing the sum of the Poynting vectors normal to each face of a cube enclosing the dipole plus the nanostructures, to the sum of the Poynting vectors when considering the dipole alone. For estimating Γ_{tot}, we calculate the energy dissipated by the dipole in the presence of the nanostructures, normalized by the one without it[30] (eq 4). This calculation implies knowledge of the dipole moment as well as the scattered field by the structures at the dipole position and therefore requires performing the same simulation twice, i.e., with and without the nanostructures, in order to estimate the scattered field.[30] The electric or magnetic Γ_{tot} are then calculated taking into account the corresponding electric or magnetic field and respective dipole moments using the following equation:

$$\Gamma_{tot} = \frac{P_{tot}}{P_0} = 1 + \frac{6\pi\varepsilon_0\varepsilon}{|\mu_A|^2}\frac{1}{k^3}\mathrm{Im}\{\mu_A A_s(r_d)\} \quad (4)$$

DOI: 10.1021/acsphotonics.5b00128
ACS Photonics 2015, 2, 1071−1076

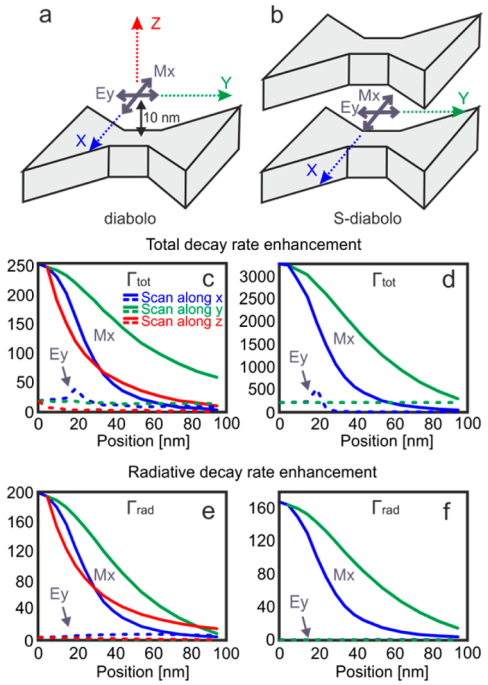

Figure 3. Total and radiative decay rate enhancements of an optical nanosource described by a magnetic or an electric dipole moment. (a, b) 3D schematics of the simulations performed; a magnetic (Mx) or an electric (Ey) dipole moment oriented along x or y, respectively, is placed in near proximity to the diabolo and S-diabolo metallic junctions (10 nm away) and scanned along (a) the x, y, z directions in the case of the diabolo and (b) x, y directions in the case of the S-diabolo. (c, d) Γ_{tot} and (e, f) Γ_{rad} for each position of these dipoles (continuous lines correspond to the magnetic dipole; dashed lines to the electric dipole) along the diabolo (c, e) and the S-diabolo (d, f).

where ε_0 and ε are respectively the vacuum permittivity and the medium relative permittivity, k is the wavenumber, and μ_A and $A_s(r_d)$ are respectively the dipole moment and the scattered field at the dipole position (the electric or magnetic ones according to the Γ_{tot} calculated).

We first addressed the influence of the antennas on the magnetic dipole. Due to the resonance properties of the antennas and their magnetic field components along x, y, and z in the near field,[22] we chose the magnetic dipole moment to emit at a wavelength of 1550 nm and to be oriented along the x-axis, which is the orientation of the magnetic field at the center of the antennas, i.e., at the metallic junction[22] (Figure 3a and b). Figure 3c and d show Γ_{tot} as a function of the dipole position for the diabolo and S-diabolo, respectively, while Figure 3e and f show their Γ_{rad} counterpart. The total decay rate of the magnetic dipole is enhanced by respectively 2 and 3 orders of magnitude for the diabolo and the S-diabolo when the dipole is centered on the metallic junction. Furthermore, the radiative decay rate is also enhanced by 2 orders of magnitude for both antennas. This result is extremely important since the radiative decay rate directly determines the amount of photons emitted in the far field by the nanosource. These are, to our knowledge, the highest theoretical decay rate (Γ_{tot} and Γ_{rad}) enhancements reported so far for a magnetic point-like emitter, making these structures highly suitable for further experimental studies.

Moreover, as observed in Figure 3c–f, both Γ_{tot} and Γ_{rad} rapidly decay when the dipole moves further away from the metallic junction. This decay is stronger along the x- and z-direction than along the y-direction, which is explained by the proximity of the metal along y continuing to influence those rates at each dipole position.[33]

To compare the influence of the resonant antennas on the enhancement of the decay rates between magnetic and electric dipoles, we performed similar studies on an electric dipole. For this, a y-oriented electric dipole is scanned along the antennas (Figure 3a and b), and for each position the values Γ_{tot} and Γ_{rad} are calculated in the same way as for the magnetic dipole presented above. Here, the electric dipole orientation is chosen to be collinear to the polarization of the resonant excitation field (Figure 2) and to the electric current (responsible for the magnetic field enhancement) running through the antenna.[22]

For both antenna configurations, at the maximum of the magnetic Γ_{tot}, its electric counterpart is more than 1 order of magnitude lower, confirming that these antennas are better suited to strongly modify the magnetic dipole emission at the nanoscale. Moreover, the ratio between electric and magnetic Γ_{rad} reduces even more due to a strong quenching of the electric dipole emission; indeed, the electric Γ_{rad} is barely present in the case of the S-diabolo (Figure 3f). As mentioned above, these calculations have been made for two specific orientations of the electric and magnetic dipoles. In order to fully cover the coupling between these antennas and such dipoles, we also calculated the averaged enhancements of Γ_{tot} and Γ_{rad} for dipoles oriented along the three main directions (x, y, z) and centered on the metallic junction, i.e, $x = y = 0$ and $z =$ 10 nm. The enhancements of the average magnetic Γ_{tot} and Γ_{rad} are then respectively 106 and 67 in the case of the diabolo and 1155 and 56 in the case of the S-diabolo. In contrast, the enhancements of the average electric Γ_{tot} and Γ_{rad} counterparts are respectively 43 and 1.9 in the case of the diabolo and 221 and 2.63 in the case of the S-diabolo. These results demonstrate once more the ability of diabolo and S-diabolo antennas to strongly influence the total and radiative magnetic dipole emission and their poor performance to modify the radiative electric dipole emission.

Having the total and the radiative decay rates, the quantum yield (η) for each position of the magnetic dipole along the two antennas can be calculated using eq 3. The results are plotted in Figure 4. Interestingly, for the diabolo antenna, η becomes very large when the dipole is centered on the antenna, with about 80% of the energy radiated in far field. These results indicate that the diabolo geometry is a very efficient optical antenna when coupled to a magnetic nanosource. Moreover, this value

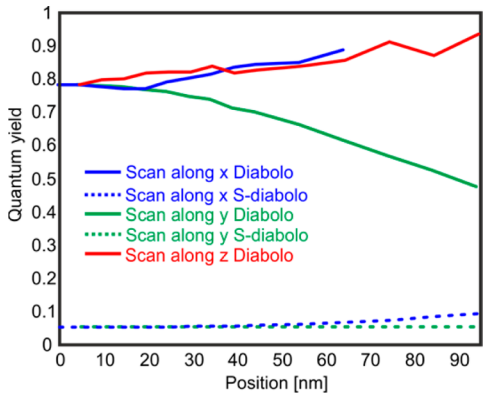

Figure 4. Quantum yield of the magnetic dipole for each spatial position for both the diabolo and the S-diabolo nanoantennas.

DOI: 10.1021/acsphotonics.5b00128
ACS Photonics 2015, 2, 1071–1076

remains rather constant when the dipole moves along the *x*- and *z*-directions and decays along the *y*-direction due to higher absorption into the metal. On the other hand, the large enhancement of the total decay rate in the case of the S-diabolo is made at the expense of a very low η of about only 5%. This makes in practice this sandwich antenna a quite inefficient system to be coupled to a magnetic dipole transition, despite its high radiative decay rate. Therefore, the use of the S-diabolo to strongly reduce the lifetime of magnetic emitters might be appropriate, but in order to enhance the fluorescence of a magnetic emitter, the diabolo configuration alone is preferred.

In addition to these results, it is worth noticing that placing an electric dipole in close proximity to the metallic junction of these two structures, aside from reducing Γ_{tot} and Γ_{rad} by more than 1 order of magnitude with respect to a magnetic dipole, it also strongly reduces η, with 20% and less than 0.1% efficiency for the diabolo and the S-diabolo, respectively.

Finally, in order to fully describe the coupling between the diabolo nanoantenna and the magnetic dipole, we performed simulations to unravel the effect of the diabolo on the MLDOS in a transversal plane 10 nm away from the diabolo (Figure 5a).

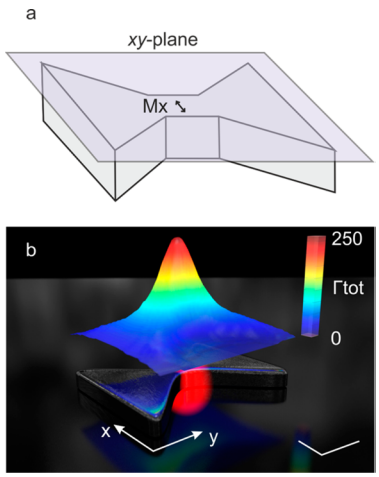

Figure 5. MLDOS mapping. (a) 3D schematic of the simulations performed; a magnetic dipole oriented along *x* is placed near the diabolo antenna (10 nm) and scanned along the *xy*-plane. At each position, Γ_{tot} is calculated. (b) 3D plot of the MLDOS superimposed to the diabolo antenna. The scale bars are 100 nm.

Figure 5b displays a three-dimensional map of the total decay rate enhancement superimposed to the diabolo nanoantenna that is directly proportional to the MLDOS.[7] Therefore, it can be clearly seen that the MLDOS is strongly affected on a very small area near the metallic junction, corresponding to the region where the magnetic field is also strongly enhanced, as shown in Figure 2a and b. This is, to our knowledge, the first theoretical mapping of the MLDOS in near proximity to a plasmonic nanoantenna. We believe that these results demonstrate the strong potential for such nanoantennas to study the properties and interactions between magnetic light and matter at the nanometer scale.

CONCLUSIONS

In summary, we have theoretically shown an increase of 2 to 3 orders of magnitude on both the total and radiative decay rates of a magnetic dipole moment by placing it in near proximity to a plasmonic nanoantenna designed to create a single magnetic hot spot at the nanometer scale. These strong enhancements have been demonstrated for both diabolo and S-diabolo antennas and are confined in a small subwavelength volume close to their metallic junction. Furthermore, we showed oppose effects of these two antennas on the quantum yield of the magnetic dipole; that is, the diabolo behaves as an efficient antenna, while the S-diabolo quenches the emission. Finally, we theoretically mapped the behavior of the MLDOS in the entire plane close to a diabolo optical nanoantenna, providing a thorough understanding of the antenna influence on a magnetic dipole transition.

These results highlight the unique ability of such optical nanoantennas to enhance and control light emission from magnetic dipole transitions in matter, for example in lanthanide ions. In particular, the proposed optical nanoantennas would be extremely well suited to study such transitions in Er^{3+}, as this ion is known to sustain a strong magnetic dipole transition[34] at the telecom wavelength and serves as an important emitter in a wide range of technological applications.

AUTHOR INFORMATION

Corresponding Author

*E-mail: mathieu.mivelle@espci.fr.

Present Address

#ESPCI ParisTech, PSL Research University, CNRS, Institut Langevin, 1 Rue Jussieu, 75005 Paris, France.

Author Contributions

The manuscript was written through contributions of all authors. All authors have given approval to the final version of the manuscript.

Notes

The authors declare no competing financial interest.

ACKNOWLEDGMENTS

The research leading to these results has received funding from the European Commission's Seventh Framework Programme under grant agreement 288263 (NanoVista).

REFERENCES

(1) Cowan, R. D. *The Theory of Atomic Structure and Spectra*; University of California Press, 1981; Vol. 3.

(2) Vahala, K. J. Optical microcavities. *Nature* **2003**, *424*, 839−846.

(3) Lodahl, P.; Van Driel, A. F.; Nikolaev, I. S.; Irman, A.; Overgaag, K.; Vanmaekelbergh, D.; Vos, W. L. Controlling the dynamics of spontaneous emission from quantum dots by photonic crystals. *Nature* **2004**, *430*, 654−657.

(4) Kühn, S.; Håkanson, U.; Rogobete, L.; Sandoghdar, V. Enhancement of single-molecule fluorescence using a gold nanoparticle as an optical nanoantenna. *Phys. Rev. Lett.* **2006**, *97*, 017402.

(5) Anger, P.; Bharadwaj, P.; Novotny, L. Enhancement and quenching of single-molecule fluorescence. *Phys. Rev. Lett.* **2006**, *96*, 113002.

(6) Purcell, E. M. Spontaneous emission probabilities at radio frequencies. *Phys. Rev.* **1946**, *69*, 681.

(7) Grynberg, G.; Aspect, A.; Fabre, C. *Introduction to Quantum Optics: From the Semi-classical Approach to Quantized Light*; Cambridge University Press, 2010.

(8) Noginova, N.; Barnakov, Y.; Li, H.; Noginov, M. Effect of metallic surface on electric dipole and magnetic dipole emission transitions in Eu^{3+} doped polymeric film. *Opt. Express* **2009**, *17*, 10767−10772.

(9) Karaveli, S.; Zia, R. Strong enhancement of magnetic dipole emission in a multilevel electronic system. *Opt. Lett.* **2010**, *35*, 3318−3320.

DOI: 10.1021/acsphotonics.5b00128
ACS Photonics 2015, 2, 1071−1076

(10) Karaveli, S.; Wang, S.; Xiao, G.; Zia, R. Time-Resolved Energy-Momentum Spectroscopy of Electric and Magnetic Dipole Transitions in Cr^{3+}: MgO. *ACS Nano* **2013**, *7*, 7165−7172.
(11) Taminiau, T. H.; Karaveli, S.; van Hulst, N. F.; Zia, R. Quantifying the magnetic nature of light emission. *Nat. Commun.* **2012**, *3*, 979.
(12) Aigouy, L.; Cazé, A.; Gredin, P.; Mortier, M.; Carminati, R. Mapping and quantifying electric and magnetic dipole luminescence at the nanoscale. *Phys. Rev. Lett.* **2014**, *113*, 076101.
(13) Karaveli, S.; Zia, R. Spectral tuning by selective enhancement of electric and magnetic dipole emission. *Phys. Rev. Lett.* **2011**, *106*, 193004.
(14) Novotny, L.; van Hulst, N. Antennas for light. *Nat. Photonics* **2011**, *5*, 83−90.
(15) Mivelle, M.; van Zanten, T. S.; Garcia-Parajo, M. F. Hybrid photonic antennas for subnanometer multicolor localization and nanoimaging of single molecules. *Nano Lett.* **2014**, *14*, 4895−4900.
(16) Singh, A.; Calbris, G.; van Hulst, N. F. Vectorial Nanoscale Mapping of Optical Antenna Fields by Single Molecule Dipoles. *Nano Lett.* **2014**, *14*, 4715−4723.
(17) Suarez, M.; Grosjean, T.; Charraut, D.; Courjon, D. Nanoring as a magnetic or electric field sensitive nano-antenna for near-field optics applications. *Opt. Commun.* **2007**, *270*, 447−454.
(18) Boudarham, G.; Abdeddaim, R.; Bonod, N. Enhancing the magnetic field intensity with a dielectric gap antenna. *Appl. Phys. Lett.* **2014**, *104*, 021117.
(19) Ginn, J. C.; Brener, I.; Peters, D. W.; Wendt, J. R.; Stevens, J. O.; Hines, P. F.; Basilio, L. I.; Warne, L. K.; Ihlefeld, J. F.; Clem, P. G. Realizing optical magnetism from dielectric metamaterials. *Phys. Rev. Lett.* **2012**, *108*, 097402.
(20) Albella, P.; Poyli, M. A.; Schmidt, M. K.; Maier, S. A.; Moreno, F.; Sáenz, J. J.; Aizpurua, J. Low-loss Electric and Magnetic Field-Enhanced Spectroscopy with Subwavelength Silicon Dimers. *J. Phys. Chem. C* **2013**, *117*, 13573−13584.
(21) García-Etxarri, A.; Gómez-Medina, R.; Froufe-Pérez, L. S.; López, C.; Chantada, L.; Scheffold, F.; Aizpurua, J.; Nieto-Vesperinas, M.; Sáenz, J. Strong magnetic response of submicron silicon particles in the infrared. *Opt. Express* **2011**, *19*, 4815−4826.
(22) Grosjean, T.; Mivelle, M.; Baida, F.; Burr, G.; Fischer, U. Diabolo nanoantenna for enhancing and confining the magnetic optical field. *Nano Lett.* **2011**, *11*, 1009−1013.
(23) Rolly, B.; Bebey, B.; Bidault, S.; Stout, B.; Bonod, N. Promoting magnetic dipolar transition in trivalent lanthanide ions with lossless Mie resonances. *Phys. Rev. B: Condens. Matter Mater. Phys.* **2012**, *85*, 245432.
(24) Hein, S. M.; Giessen, H. Tailoring Magnetic Dipole Emission with Plasmonic Split-Ring Resonators. *Phys. Rev. Lett.* **2013**, *111*, 026803.
(25) Choi, Y.; Choi, D.; Lee, L. P. Metal−Insulator−Metal Optical Nanoantenna with Equivalent-Circuit Analysis. *Adv. Mater.* **2010**, *22*, 1754−1758.
(26) Roden, J. A.; Gedney, S. D. Convolutional PML (CPML): An efficient FDTD implementation of the CFS-PML for arbitrary media. *Microw. Opt. Technol. Lett.* **2000**, *27*, 334−338.
(27) Pakizeh, T.; Abrishamian, M.; Granpayeh, N.; Dmitriev, A.; Käll, M. Magnetic-field enhancement in gold nanosandwiches. *Opt. Express* **2006**, *14*, 8240−8246.
(28) Pakizeh, T.; Dmitriev, A.; Abrishamian, M.; Granpayeh, N.; Käll, M. Structural asymmetry and induced optical magnetism in plasmonic nanosandwiches. *J. Opt. Soc. Am. B* **2008**, *25*, 659−667.
(29) Curto, A. G.; Volpe, G.; Taminiau, T. H.; Kreuzer, M. P.; Quidant, R.; van Hulst, N. F. Unidirectional emission of a quantum dot coupled to a nanoantenna. *Science* **2010**, *329*, 930−933.
(30) Novotny, L.; Hecht, B. *Principles of Nano-optics*; Cambridge University Press, 2012.
(31) Taminiau, T.; Stefani, F.; Segerink, F.; Van Hulst, N. Optical antennas direct single-molecule emission. *Nat. Photonics* **2008**, *2*, 234−237.
(32) Kaminski, F.; Sandoghdar, V.; Agio, M. Finite-difference time-domain modeling of decay rates in the near field of metal nanostructures. *J. Comput. Theor. Nanosci.* **2007**, *4*, 635−643.
(33) Chance, R.; Prock, A.; Silbey, R. Molecular fluorescence and energy transfer near interfaces. *Adv. Chem. Phys.* **1978**, *37*, 65.
(34) Li, D.; Jiang, M.; Cueff, S.; Dodson, C. M.; Karaveli, S.; Zia, R. Quantifying and controlling the magnetic dipole contribution to 1.5−μ m light emission in erbium-doped yttrium oxide. *Phys. Rev. B: Condens. Matter Mater. Phys.* **2014**, *89*, 161409.

DOI: 10.1021/acsphotonics.5b00128
ACS Photonics 2015, 2, 1071−1076